16th International Congress of the Geological Society of Greece

17-19 October, 2022 - Patras, Greece

Bulletin of the Geological Society of Greece, Sp. Publ. 10

Ext. Abs. GSG2022-181

Investigating the capability of Sentinel-2 and Worldview-3 SWIR to map the main mineralogical composition of bauxite through spectral unmixing. Case Study: Itea, Greece.

A. Anifadi[1,2], O. Sykioti[3], K. Koutroumbas[3], E. Vassilakis[2], E. Georgiou[4], C. Vasilatos[2]

(1) Faculty of Geology & Geoenvironment, National and Kapodistrian University of Athens, Athens, Greece (2) LARCO GMM S.A., Greece (3) Institute of Astronomy, Astrophysics, Space Applications and Remote Sensing, National Observatory of Athens, Athens, Greece, sykioti@noa.gr (4) Titan Cement Co. S.A., Athens, Greece

Introduction and Objectives

During the last decades, geological remote sensing, including hyperspectral/multispectral data, has grown rapidly in applications such as mineral/ore exploration and mineral resource mapping (Anifadi *et al.*, 2022; Anifadi *et al.*, 2019; van der Meer *et al.*, 2014). Sentinel-2 (S-2) (12 spectral bands within the VNIR-SWIR region of the H/M spectrum), has added new significant capabilities in terms of spatial resolution and spectral information, especially in the VNIR region (Burns, 1993; Clark and Roush, 1984). In parallel, DigitalGlobe's Worldview-3 (WV3) satellite provides very high spatial resolution (1.24m/pixel in the VNIR and 3.7m/pixel in the SWIR) and eight SWIR bands with valuable information on mineralogy, especially on alteration.

Spectral unmixing (SU) is a well-known image processing method at sub-pixel level. The aim of SU is the decomposition of the spectral signatures of mixed pixels into a selection of spectral signatures (represented as vectors) corresponding to the reflectance of pure physical materials (endmembers) (Keshava, 2003). SU results in a set of fractions (abundances) images, which indicate the degree of presence of each endmember within each pixel. Although several SU approaches have been proposed in literature, when working with multispectral data, the most widely used are those adopting the linear mixing model, where the spectral signature (vector) of each pixel is assumed to be expressed as a linear combination of a set of endmember signatures (vectors). The coefficients (abundances) of this combination can be estimated through various unmixing procedures, such as the constrained/unconstrained least squares methods. The objective of this study is to investigate the potential of the capability of S-2 and WV3-SWIR through linear SU to detect minerals which are typical to a bauxite composition. The study is conducted on two selected stock piles of bauxite in the transport zone in Itea Greece.

Data and analysis

For the purpose of this study, two satellite images were utilized, a S-2 image acquired in 3/7/2018 and a WV3-SWIR image acquired in 26/06/2015. Both datasets were georeferenced and atmospherically corrected. All spectral bands of the S-2 output reflectance image were resampled to 10m spatial resolution. The WV-3 SWIR image was co-registered to the S-2 image. Two subset images were then extracted using two Regions of Interest (ROIs) delineating two bauxite stock piles (Fig. 1a,b), named hereafter as A1 and A2. The number of pixels that are included within A1 is 10 for S-2 and 51 for the WV-3 SWIR image and the corresponding number of pixels included within A2 is 8 for S-2 and 36 for the WV-3 SWIR image. Next, five minerals were selected as typical of greek bauxites composition (Mondillo *et al.*, 2022), namely diaspore, goethite, hematite, anatase and kaolinite (there is no available spectral signature of boehmite and quartz is almost featureless in the two datasets spectral bands). The spectral signatures of the five minerals were retrieved from the USGS Spectral Library, convolved to the S-2 and WV3-SWIR spectral bands. The five spectral signatures of each dataset (Fig. 2a, b) were used as endmembers in SU. We performed (i) unconstrained (UC) linear SU and (ii) linear SU with non-negativity constraint (NNG) (the sum-to-one constraint SU and the non-negativity and sum-to-one constraint SU both failed to provide realistic results). The abundance values of the (i) and (ii) SU procedures were calculated for each endmember and each pixel of each one of the two datasets. The larger (positive) the abundance values are, the more indicative of the mineral's presence within the pixel are. For each pixel of each area, its abundance values were normalized in order to sum to one. We then calculated the mean abundance value for each mineral for each study area and the corresponding standard deviation.

Discussion and Conclusions

In general, the results obtained by SU UC and SU NNG methods are consistent to each other, in the sense that the numerical ordering between the abundance values of two minerals is the same for the two datasets and for both areas. For each area, the processing of both datasets resulted in high presence of diaspore (main bauxite mineral), especially for S-2 (>0.80). In all cases, the relatively low standard deviation values of diaspore (<0.11) indicate its uniform presence within each area, in contrast to the corresponding distribution of the other minerals, especially the iron-bearing ones. Furthermore, in the case of S-2, diaspore seems to prevail to the iron phases (goethite <0.19, hematite <0.28) while in the case of WV3 SWIR, the difference between diaspore and iron minerals abundances is not so sharp (diaspore >0.30 reaching 0.46 in the case NNG, goethite >0.30, hematite <0.31). However, in contrast to S-2, WV3-SWIR is capable to detect the presence of all five minerals, even if it is weak (e.g. kaolinite <0.0003), with the exception of anatase in A2 which is not detected.

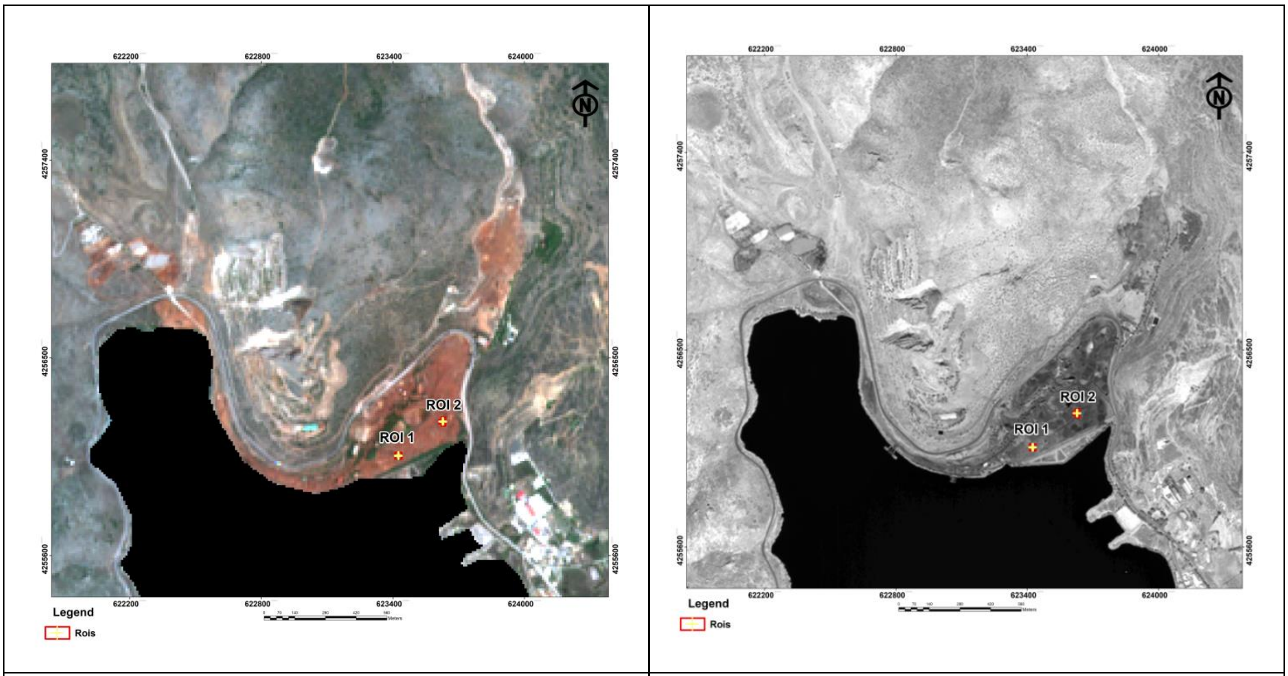

(a) (b)

Figure 1. Location of the two bauxite stock piles under study (ROI1, ROI2 in yellow crosses) on (a) the true color composition of the S-2 image; (b) on a pseudo-color composition of the WV3-SWIR image.

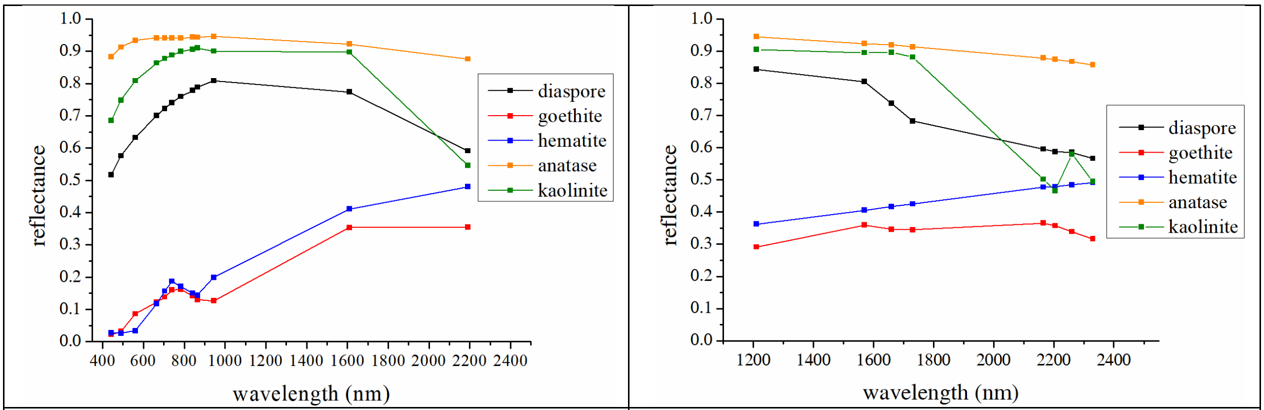

(a) (b)

Figure 2. Plot of the five endmembers used in the SU procedure on the a) S-2 and b) WV3-SWIR spectral bands.

References

Anifadi, A., Sykioti, O., Koutroumbas, K., Vassilakis, E., 2022. A Novel Spectral Index for Identifying Ferronickel (Fe–Ni) Laterites from Sentinel 2 Satellite Data. Natural Resources Research 31, 1203-1244.

Anifadi, A., Sykioti, O., Vassilakis, E., 2019. Detection of chromite minerals using Spectral Linear Unmixing on Sentinel-2 imagery. Case study: Ingessana Hills, Blue Nile Province, Soudan. 15th International Congress of the Geological Society of Greece, Athens, Greece, 199.

Burns, R.G., 1993. Mineralogical Applications of Crystal Field Theory. 2nd Ed. Cambridge University Press.

Clark, R.N., Roush, T.L. 1984. Reflectance spectroscopy—quantitative analysis techniques for remote sensing applications. Journal of Geophysical Research 89, 6329–6340.

Keshava, N. 2003. A survey of spectral unmixing algorithms. Lincoln Laboratory Journal 14 (1), 55–78.

Mondillo, N., Di Nuzzo, M. , Kalaitzidis, S., Boni, M, Santoro, L., Balassone G., 2022. Petrographic and geochemical features of the B3 bauxite horizon (Cenomanian-Turonian) in the Parnassos-Ghiona area: A contribution towards the genesis of the Greek karst bauxites. Ore Geology Reviews 143, 104759.

Van der Meer, F.D., Van der Werff, H.M.A., van Ruitenbeek, F.J.A. 2014. Potential of ESA's Sentinel-2 for geological applications. Remote Sensing of Environment 148, 124-133.